Comparative Study of Air-Gap Field Distribution Characteristics Among Different Pole Array in SPM

Xinghua He[1], Liang Yan[1,2,3(✉)], Xiaoshan Gao[1], Pengjie Xiang[1], and Chris Gerada[4]

[1] School of Automation Science and Electrical Engineering, Beihang University, Beijing 100191, China
lyan1991@gmail.com

[2] Science and Technology on Aircraft Control Laboratory, Beihang University, Beijing 100191, China

[3] Ningbo Institute of Technology, Beihang University, Ningbo 315800, China

[4] Power Electronics, Machines and Control Group, University of Nottingham, Nottingham NG7 2RD, UK

Abstract. The pole array directly influences air-gap filed distribution and hence output torque performance especially in surface-mounted PM machine (SPM). The fundamental wave of air-gap magnetic flux density determines the average torque, and harmonic generates torque ripple. In generally, there is a trade-off between them. To simultaneously obtain high torque and low torque ripple, the selection of pole array and corresponding design parameters is essential for PM machine design. Thus, the air-gap field distribution characteristics of three kinds of pole arrays, i.e., radial-magnetized, tangential-magnetized and Halbach array are analysed and compared by finite element analysis (FEA). The effects of the pole arc coefficient and PM thickness coefficient on air-gap field distribution are analysed by fast Fourier transform (FFT). It indicates that the effects of the pole arc length on the harmonic component of air gap magnetic field is obvious and the effects of the pole thickness is very little. The performances of three pole arrays under different pole thicknesses are compared. The results show that radial-magnetized pole array perform better than Halbach array and tangential-magnetized pole array on fundamental flux density when thickness of magnetic pole is small. Besides, when the thickness of magnetic pole exceeds 0.9 times of pole distance, tangential-magnetized pole array can obtain higher fundamental magnetic density than Halbach array.

Keywords: Surface-mounted · Brushless Torque Motor · Harmonic Analysis · Magnetic Pole Array · Finite Element Analysis

1 Introduction

Brushless torque motors are widely used in electric power steering, robotics, etc. [1]. Generally, large number of poles, large split ratio of stator and surface-mounted rotor

L. Yan and J. Na (Eds.): ICFPMCE 2022, AHE 10, pp. 202–213, 2023.
https://doi.org/10.2991/978-94-6463-022-0_18

are used in a brushless torque motor. The torque characteristics of surface mounted PM motor are mainly determined by the air-gap magnetic field generated by the rotor pole. It has been proved that the fundamental wave of radial magnetic density in the air gap determines the average torque of the motor. For three-phase motor, the third harmonic has no contribution to the torque. However, other high-order harmonics can cause torque ripple, of which the fifth and seventh harmonics wave play the most serious role. Besides, the radial magnetic density waveform of the air gap is extremely influenced by the magnetic pole array of the rotor.

At present, the most commonly used magnetic pole array is radial-magnetized pole array [2–4], which is widely used because of its simple manufacture and assembly process. Since the appearance of Halbach array [5], it has been used in torque motor and achieved good results because of its high fundamental magnetomotive force and magnetic shielding characteristics [6, 7]. Recently, scholars have found that tangential-magnetized pole array or spoke-type rotor can obtain higher fundamental magnetic flux density in air gap [8, 9], and the soft magnetic material between magnetic poles also makes it possible for field weakening control. Therefore, the output torque and flexibility of motor control increases. However, most scholars only study specific arrays, and few compare and analyse the three magnetic pole arrays, so as to guide the selection of magnetic pole array in practical engineering application.

In this paper, the above three kinds of magnetic pole arrays are studied. For different pole arc pole arc length and pole thickness, the air-gap radial magnetic density waveform is analysed. Finally, above three different magnetic pole arrays are compared to be a reference to select appropriate magnetic pole arrays.

In this paper, the remainder is organized as follows. In Sect. 2, parameterized finite element simulation model of three pole arrays is established. In Sect. 3, the FEA of three kinds of magnetic pole arrays under different pole arc length and magnetic pole thickness is carried out, and the influence of magnetic pole structure parameters on air-gap magnetic density is analysed by FFT. In Sect. 4, the output characteristics of three magnetic pole arrays under the same mass is compared. Finally, the study is concluded in Sect. 5.

2 Parametric Simulation Model

Because the split ratio of torque motor is large, and it has many pole pairs, the magnetic pole surface is close to a straight line. Thus, the rotor magnetic pole can be expanded into a straight line for research. The geometric model in one period is shown in Fig. 1, where τ is the pole pitch; h is the pole thickness; and b is the pole arc length. For a specific number of slots and poles, the pole pitch remains unchanged. In order to make the simulation results universal, the pole arc length b and pole thickness h are nondimensionalized based on the pole pitch. The ratio of pole arc to pole pitch or pole embrace coefficient is defined as

$$a_p = \frac{b}{\tau} \tag{1}$$

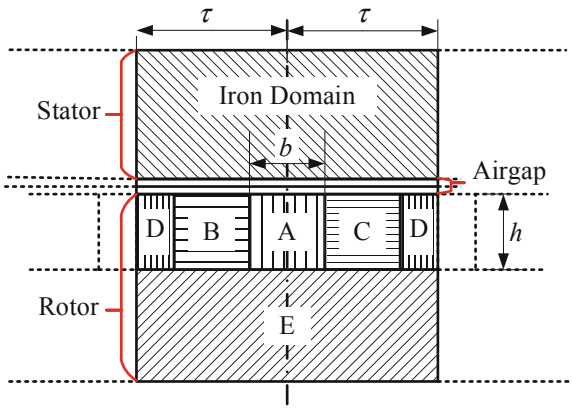

Fig. 1. Geometric model for the simulation.

The pole thickness coefficient is defined as

$$a_h = \frac{h}{\tau} \tag{2}$$

The air-gap length in this model is 1 mm. Pole pitch τ is 10 mm. According to Eq. (1) and (2), The magnetic pole arc length and pole thickness are calculated by the following:

$$\begin{cases} b = a_p \tau \\ h = a_h \tau \end{cases} \tag{3}$$

The stator is made of iron. The rotor is divided into five regions. In order to simulate three magnetic pole arrays in one geometric model, the material distribution and magnetization direction of the five regions are shown in Table 1. The arrow ($\uparrow\downarrow\leftarrow\rightarrow$) represents the magnetization direction, and also indicates that the material is permanent magnet.

The material and magnetization directions are distributed according to the characteristics of three types of magnetic pole arrays. The distribution principle is to maximize its performance and ensure the rationality of comparison. For example, there is no back iron for tangential-magnetized pole array and no iron between radial-magnetized poles so that the magnetic circuit will go through the air gap and be prevent from invalid circulation. Besides, the Halbach array is also has no back iron so that it is convenient to compare with tangential-magnetized pole array under same mass.

Table 1. Material and Magnetization Distribution

Domain	Radial-Magnetized	Halbach Array	Tangential-Magnetized
A	↑	↑	Iron
B	Air	→	→
C	Air	←	←
D	↓	↓	Iron
E	Iron	Air	Air

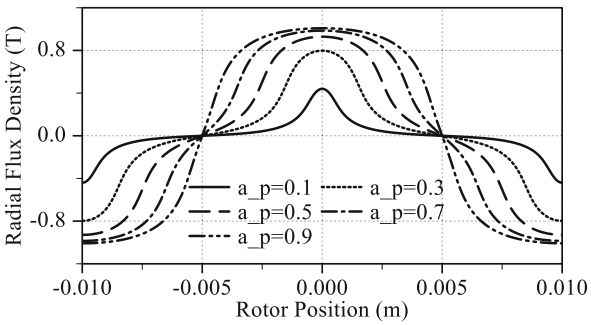

Fig. 2. Air-gap flux density waveforms under different pole embrace coefficient.

3 Air Gap Magnetic Field Analysis

3.1 Radial-Magnetized Array

Setting the pole thickness coefficient to 0.5, the air-gap flux density waveform under different pole embrace coefficient is shown in Fig. 2. With the increase of the coefficient, the waveform becomes wider, and finally approaches the square wave. This trend is obvious and predictable. Figure 3 shows The FFT results of the air-gap magnetic flux density waveform. In order to facilitate observation, double Y-axis display is adopted. The coordinate axes of fundamental wave and third harmonic are on the left, and the coordinate axes of fifth and seventh harmonic are on the right. It can be seen from Fig. 3 that the harmonic is extremely impacted by the pole embrace coefficient. With the increasing of this coefficient, the fundamental wave continuously increases, and the harmonic changes periodically. The change periods of the third, fifth as well as seventh harmonics are 2/3, 2/5 and 2/7 respectively. When the ratio is a multiple of the change.

period, the corresponding harmonic becomes very little. Therefore, the pole embrace coefficient of radial-magnetized motors is recommended within 0.8–0.857.

When setting the pole embrace coefficient to 1/2, the waveform under different pole thickness coefficient is shown in Fig. 4. Likewise, the FFT results of the waveform are shown in Fig. 5. They show that the effect of pole thickness coefficient on harmonic is

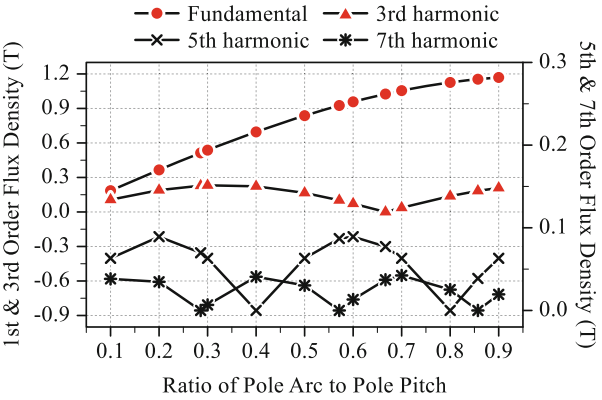

Fig. 3. Air-gap harmonic flux density under different pole embrace coefficient.

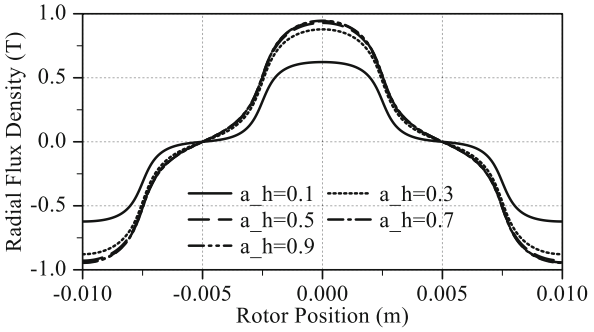

Fig. 4. Air-gap flux density waveforms under different pole thickness coefficient.

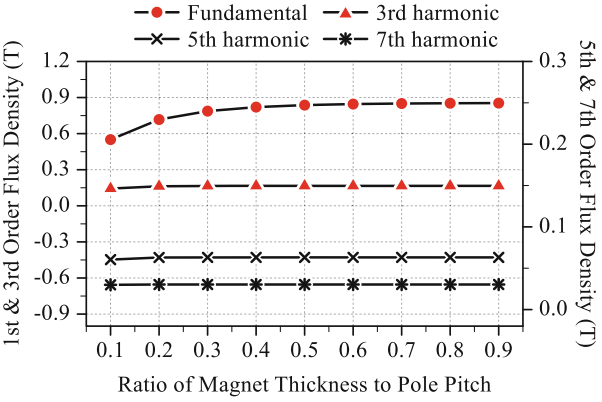

Fig. 5. Air-gap harmonic flux density under different pole thickness coefficient.

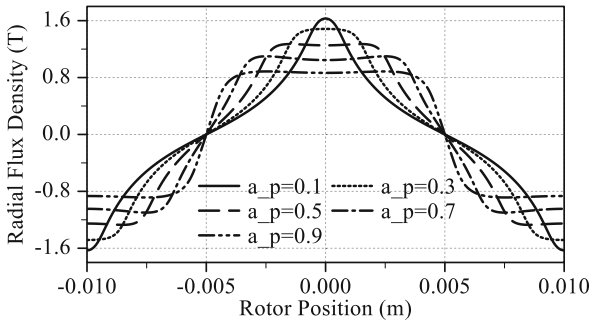

Fig. 6. Air-gap flux density waveforms under different pole embrace coefficient.

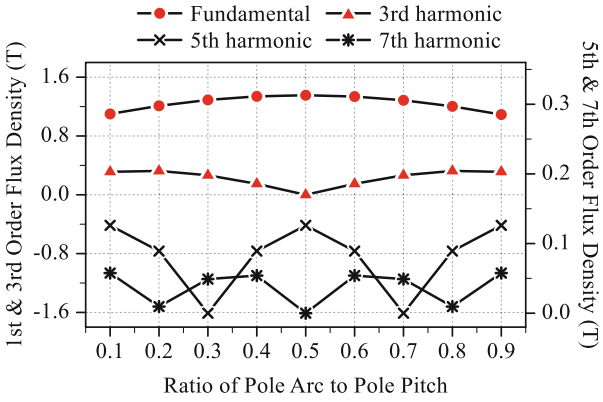

Fig. 7. Air-gap harmonic flux density under different pole embrace coefficient.

very little. With the increase of this coefficient, it is found that the peak of waveform and fundamental wave grows, and the growth rate is decreasing.

3.2 Halbach Array

Setting the pole thickness coefficient to 0.5, the waveform under different pole embrace coefficient of the air-gap magnetic flux density is shown in Fig. 6. With the increase of this ratio, the waveform becomes wider, while the peak decreases. The FFT results of the waveform are shown in Fig. 7. The graphs seem perfectly symmetrical. When the ratio is 0.5, the fundamental wave is the biggest and the third and seventh harmonic wave is almost zero. When pole embrace coefficient is 0.3 and 0.7, the fifth harmonic wave is almost zero. Comparing with the radial-magnetized poles, The fundamental magnetic flux density of Halbach array is higher, which is the reason why it can improve torque density of motor.

Setting the pole embrace coefficient to 0.5, the waveform of the air-gap magnetic flux density and its FFT results under different pole thickness coefficients is shown in Fig. 8 and Fig. 9 respectively. it can be found that with the increase of pole thickness coefficient, the fundamental wave grows but there is almost no effect on harmonic.

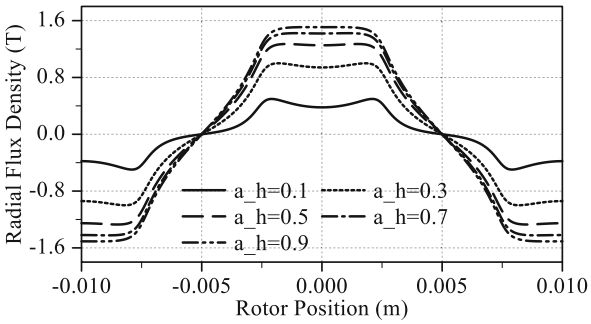

Fig. 8. Air-gap flux density waveforms under different pole thickness coefficient.

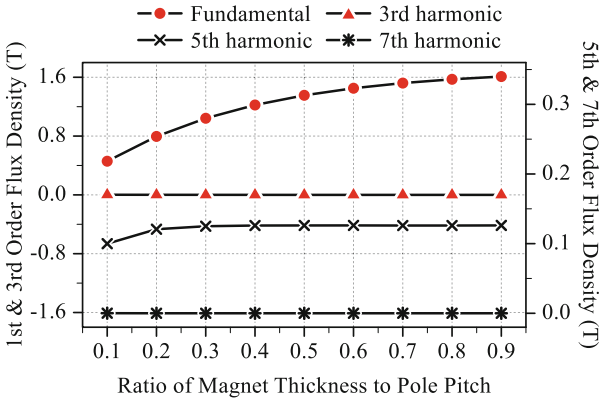

Fig. 9. Air-gap harmonic flux density under different pole thickness coefficient.

3.3 Tangential-Magnetized Array

The waveform of the air-gap magnetic flux density under different pole embrace coefficient with the pole thickness coefficient of 0.5 is shown in Fig. 10. With the increase of this coefficient, the waveform becomes wider, while the peak decreases. The FFT results of the waveform are shown in Fig. 11. It seems the same as Halbach array, but not symmetrical. This may because the iron between magnet is saturated. The fundamental wave is strictly decreasing with the increase of this coefficient if the iron not saturated. But in practice, as shown in Fig. 11, there is a peak on the fundamental wave in the graph due to the saturation of iron.

The waveform of the air-gap magnetic flux density and its FFT results under different pole thickness coefficients with pole embrace coefficient of 0.5 is shown in Fig. 12 and Fig. 13 respectively. With the increase of pole thickness coefficient, the fundamental and fifth harmonic waves grow but there is no effect on third and seventh harmonic.

Because of the nonlinearity of iron materials, the magnetoresistance of the iron between magnets grows along with the increase of magnetic density. With the pole thickness increasing, the magnetic density enlarges which cause the saturation of iron. Therefore, the pole arc coefficient corresponding to the maximum fundamental wave is

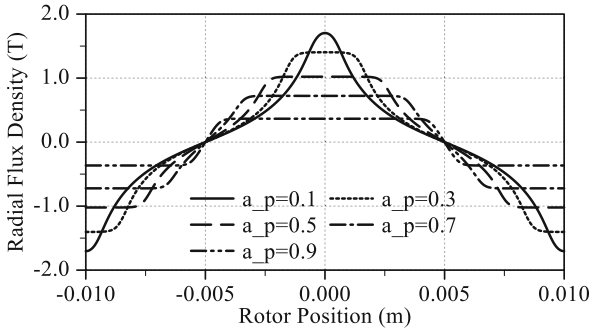

Fig. 10. Air-gap flux density waveforms under different pole embrace coefficient.

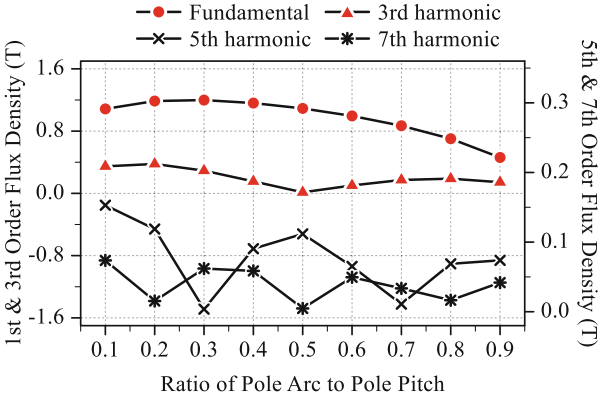

Fig. 11. Air-gap harmonic flux density under different pole embrace coefficient.

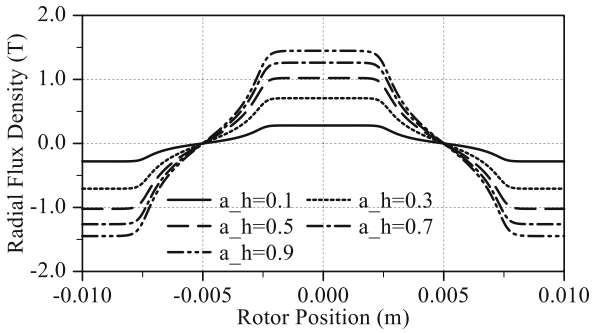

Fig. 12. Air-gap flux density waveforms under different pole thickness coefficient.

different under different pole thickness. To illustrate this relationship, a 2D contour map is made. As shown in Fig. 14, it seems that with the increasing of the pole thickness coefficient, the pole embrace coefficient should also increase to make the fundamental wave as large as possible.

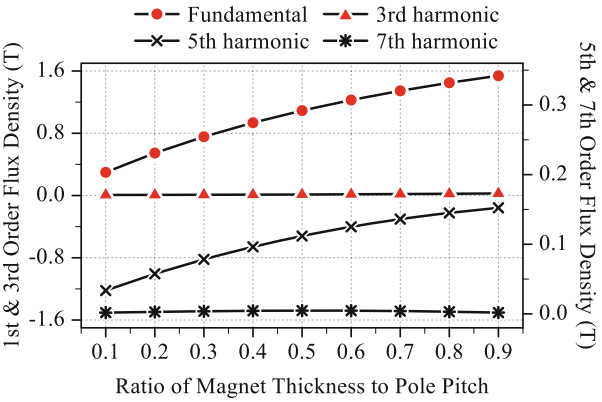

Fig. 13. Air-gap harmonic flux density under different pole thickness coefficient.

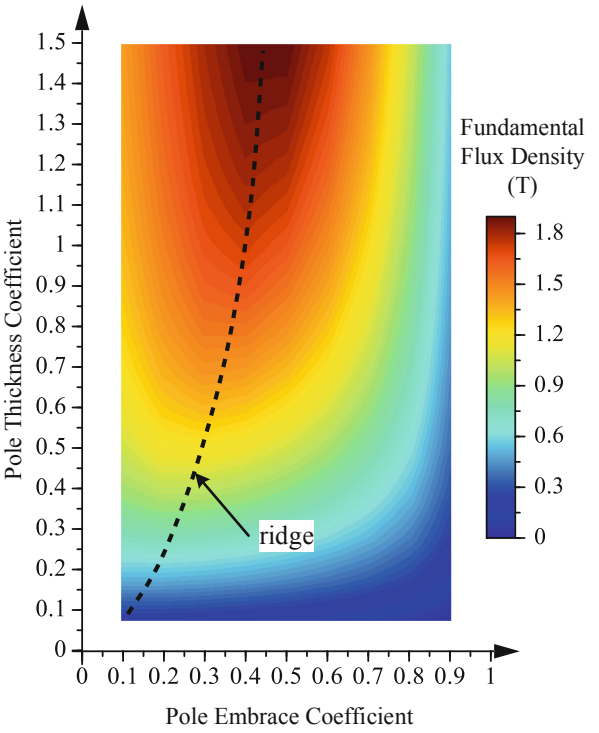

Fig. 14. Air-gap fundamental flux density under different pole embrace and pole thickness coefficient.

4 Pole Array Comparison

From the previous simulation results, the pole thickness coefficient has little influence on harmonics, while the pole embrace coefficient has a great influence. By selecting

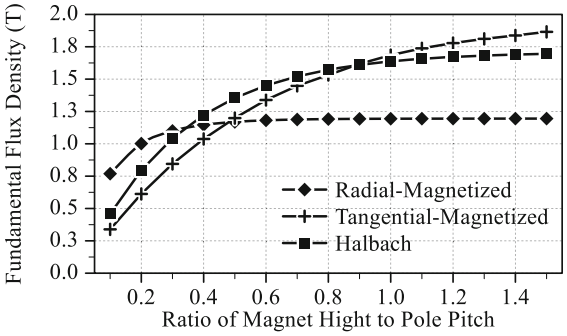

Fig. 15. Air-gap fundamental flux density under different pole thickness coefficient.

appropriate pole embrace coefficient, the harmonic component can be reduced, and then the torque ripple can be weakened. However, to improve the torque density of the motor, the fundamental magnetic density should be especially focused. In order to compare the fundamental air-gap magnetic flux density amplitudes of these three pole arrays under the same mass, the maximum fundamental magnetic density under different pole thickness is compared, and the results are shown in the Fig. 15. Because the effects of pole embrace coefficient and pole thickness coefficient on air-gap flux density harmonics are independent of each other for radial-magnetized pole array and Halbach array, it is reasonable to choose a good pole embrace coefficient and then only study the influence of pole thickness on fundamental magnetic field. Here, the pole embrace coefficient of radial-magnetized pole array is 0.9, and that of Halbach is 0.5. The polar arc coefficient and height coefficient of tangential-magnetized pole array are coupled together, so the data are obtained according to the ridge line in Fig. 15. The results show that:

1. The growth rate of radial-magnetized pole array and Halbach array slows down with the increase of pole thickness coefficient;
2. The fundamental magnetic density of radial-magnetized pole array is greater than that of Halbach array and tangential-magnetized pole array when the thickness of magnetic pole is small;
3. When the thickness of magnetic pole exceeds 0.9 times of pole distance, tangential-magnetized pole array can obtain higher fundamental magnetic density than Halbach array.

5 Conclusion

In order to provide a basis for the selection of appropriate pole arrays, three pole arrays such as radial-magnetized, tangential-magnetized and Halbach array are analysed by FEA. The effects of the pole embrace and pole thickness on air-gap magnetic field are studied by FFT of the magnetic density waveform. Finally, the performances of three pole arrays under different pole thicknesses are compared. The main conclusions are as follows:

1. The effects of the pole embrace coefficient on the harmonic component of air-gap magnetic field is obvious and the effects of the pole thickness is very little.
2. Under certain pole embrace coefficient, the fifth and third harmonics can be eliminated.
3. Radial-magnetized pole array performs better than Halbach array and tangential-magnetized pole array on fundamental flux density when thickness of magnetic pole is small.
4. When the thickness of magnetic pole exceeds 0.9 times of pole distance, tangential-magnetized pole array can obtain higher fundamental magnetic density than Halbach array.

Acknowledgments. This research was funded by the National Natural Science Foundation of China (NSFC) under grant 52130505 and 51875013, the National Key R&D Program under grant 2022YFE0113700, the Ningbo key scientific and technological project under grant 2022Z040, National Defense Science and Technology Key Laboratory Foundation under grant JSY6142219202109, and Fundamental Research Funds for the Central Universities.

Authors' Contributions. Conceptualization, Xinghua He and Liang Yan;
Methodology, Pengjie Xiang and Liang Yan;
Software, Pengjie Xiang;
Validation, Xinghua He and Chris Gerada;
Formal analysis, Xiaoshan Gao;
Investigation, Xinghua He;
Resources, Xinghua He;
Data curation, Xiaoshan Gao;
Original draft preparation, Xinghua He;
Review and editing, Xinghua He, Liang Yan, Xiaoshan Gao, Pengjie Xiang and Chris Gerada;
Visualization, Pengjie Xiang;
Supervision, Liang Yan;
Project administration, Xiaoshan Gao;
Funding acquisition, Liang Yan.

References

1. Islam, M.S., Mir, S., Sebastian, T.: Issues in reducing the cogging torque of mass-produced permanent-magnet brushless DC motor. IEEE Trans. Ind. Appl. **40**(3), 813–820 (2004). https://doi.org/10.1109/TIA.2004.827469
2. Li, Y., Zou, J., Lu, Y.: Optimum design of magnet shape in permanent-magnet synchronous motors. IEEE Trans. Magn. **39**(6), 3523–3526 (2003). https://doi.org/10.1109/TMAG.2003.819462
3. Wang, K., Zhu, Z., Ombach, G.: Torque enhancement of surface-mounted permanent magnet machine using third-order harmonic. IEEE Trans. Magn. **50**(3), 104–113 (2013). https://doi.org/10.1109/TMAG.2013.2286780

4. Wang, K., Gu, Z., Zhu, Z., Wu, Z.: Optimum injected harmonics into magnet shape in multiphase surface-mounted PM machine for maximum output torque. IEEE Trans. Industr. Electron. **64**(6), 4434–4443 (2017). https://doi.org/10.1109/TIE.2017.2669888
5. Halbach, K.: Design of permanent multipole magnets with oriented rare earth cobalt material. Nucl. Inst. Methods **169**(1), 1 (1980). https://doi.org/10.1016/0029-554X(80)90094-4
6. Zhu, Z., Howe, D.: Halbach permanent magnet machines and applications: a review. IEE Proc.-Electr. Power Appl. **148**(4), 299–308 (2001). https://doi.org/10.1049/ip-epa:20010479
7. Duan, L., Lu, H., Zhao, C., Shen, H.: Influence of different halbach arrays on performance of permanent magnet synchronous motors. In: 2020 IEEE International Conference on Artificial Intelligence and Computer Applications (ICAICA), pp. 994–998. IEEE (2020). https://doi.org/10.1109/ICAICA50127.2020.9182625
8. Li, J., Wang, K.: A novel spoke-type PM machine employing asymmetric modular consequent-pole rotor. IEEE/ASME Trans. Mechatron. **24**(5), 2182–2192 (2019). https://doi.org/10.1109/TMECH.2019.2931950
9. Zhang, H., Hua, W., Wu, Z.: Modular spoke-type permanent-magnet machine for in-wheel traction applications. IEEE Trans. Industr. Electron. **65**(10), 7648–7659 (2018). https://doi.org/10.1109/TIE.2018.2803724